L. Bouksim and C. Bathias**

Initiation and Propagation of Short Cracks in an Aluminium Alloy Subjected to Programmed Block Loading

REFERENCE Bouksim, L. and Bathias, C., **Initiation and Propagation of Short Cracks in an Aluminium Alloy Subjected to Programmed Block Loading**, *The Behaviour of Short Fatigue Cracks*, EGF Pub. 1 (Edited by K. J. Miller and E. R. de los Rios) 1986, Mechanical Engineering Publications, London, pp. 513–526.

ABSTRACT The initiation and propagation of microcracks have been studied in 7175 T7351 aluminium alloy using 100 × 20 × 10 mm smooth test pieces subjected to three point bending. It has been shown that the initiation, determined by an acoustic emission method and corresponding to a 200 μm crack, involves a not negligible amount of crack propagation. The loading pattern chosen is a ground–air–ground spectrum consisting of two loadings each with a constant amplitude of stress ratio R = 0 and 0.7. The number of small cycles (n) of low amplitude and high R ratio per block, is variable. The experimental crack growth rate data can explain the influence of the small cycles in a block and also their influence on the propagation of short cracks of the scale of the grain size.

Introduction

In 1975, Pearson (**1**) examined short cracks in aluminium alloys. Whilst in 1979 Topper (**2**) and Kim (**3**) studied steel. This was followed by Lankford (**4**)(**5**) and other authors (**6**)–(**8**) who showed that, for a single material, if the propagation rate of long cracks conforms to the Paris law then this was not the behaviour of small fatigue cracks whose growth can take place below the threshold stress intensity factor of long cracks and whose propagation rates could be slower, and even stopped contrary to expectations based on linear elastic fracture mechanics (LEFM). The growth of these kinds of short cracks cannot, therefore, be forecast on the basis of LEFM.

The above mentioned authors hinted that the local microplasticity caused quick propagation, but that the presence of grain boundaries in plastically deformed areas created a transitory deceleration and some arrests in crack propagation. In order to understand the physical conditions that occur when the material is being damaged, we translated the problem of the initiation of a crack into the nucleation phase of a microcrack followed by the propagation of a short crack limited to 200 μm in length on the surface; this value has been chosen as an initiation criterion which can be detected by acoustic emission and has been considered acceptable technologically.

Several papers (**9**)–(**13**) on the initiation of fatigue cracks under a given load

* Laboratoire de Mécanique de l'UA 849 du CNRS – Université de technologie de Compiègne, France.

spectrum were used as a basis for this investigation, whose object is to answer the following questions

(1) How is a fatigue crack initiated under programmed block loading?
(2) What are the parameters to consider in order to model the initiation process under programmed block loading?
(3) How can the accumulation of damage under programmed block loading be expressed?

Mode of operation

The material studied was a 7175 T7351 aluminium alloy which is often used for thick pieces in aeronautical structures because of its good mechanical properties, particularly, resistance to fatigue, tensile strength, etc. The chemical constitution (% wt) was 0.08 Si, 0.17 Fe, 1.48 Cu, 2.64 Mg, 0.07 Mn, 0.19 Cr, 5.94 Zn and 0.04 Ti.

The mechanical properties of the material are, in the (L) longitudinal direction 456 MPa yield stress, 532 MPa tensile strength, and 10 per cent elongation to fracture. The corresponding data in the (T) Transverse direction were, respectively, 428 MPa, 505 MPa, and 9.4 per cent.

The microstructure as revealed by a Keller etching agent is shown in Fig. 1. The main directions are marked with the letters 'LD' (longitudinal direction), 'TD' (transverse direction), and 'ND' (normal direction); the size of the grains according to these three directions is estimated at 500 μm, 200 μm, and 20 μm, respectively. The test pieces were machined in the longitudinal direction so that the crack propagated in the normal direction. The specimen were three point bend smooth test bars measuring 100 × 20 × 10 mm.

The bending area was polished mechanically with abrasive paper, followed by aluminium oxide of 0.3 μm size and finally the specimen was given an electrolytic polishing with a buffer. The type of loading chosen was a repeated single spectrum typical of those found for aeroplanes (see Fig. 4). It consists of a ground–air–ground cycle having a zero loading for the stress at 'ground' level and a high stress at the 'air' level, e.g., $R = 0$. At the 'air' level, lower stress amplitude cycles, but with a high R ratio of 0.7, are added to simulate the perturbations during the flight of the aeroplane. During 'air flight' the maximum stress level attained is the same as that in the ground to air cycle. This spectrum is named n, with n being the number of small cycles with a high R ratio; n has a value 1, 5, 20, or 80 in the current tests. All the fatigue tests were made at room temperature on electrohydraulically pilot-operator machines of the Mayes brand. The machine is operated and controlled with the help of an external controller, either a PDP 11/10 digital microcomputer or an Apple II microcomputer. All the tests were at 10 Hz frequency.

The detection of the initiation of fatigue cracks is made with an acoustic

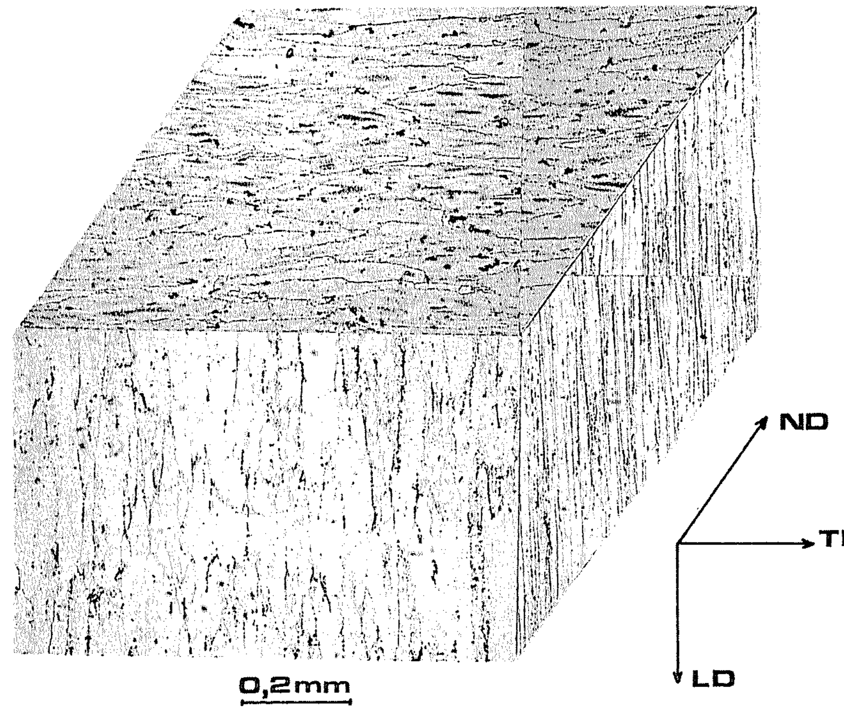

Fig 1 7175 T 7351 alloy; a three dimensional appreciation of the microstructure

emission instrument which consists of a pick up on the surface of the specimen. A preamplifier set below the pick up enables the matching of the impedence; the whole is connected with the aquisition chain of the signal (**14**). The initiation detected by acoustic emission corresponds to a semi-elliptical crack about 200 μm long. It should also be noted that the technique of plastic replication was used to observe the initiation and the propagation of short cracks until the cracks was 200 μm long. Such cellulose acetate replicas have also been used by Dowling (**15**) on A 533 B steel smooth test pieces.

The three point bending tests have been carried out with a maximum stress of 365 MPa and R ratio of 0.7 for the small cycles and R equal to 0.01 for the basic cycles. The tests are frequently interrupted while the maximum stress value is maintained in order to take prints from the surface of the damaged specimen. The replicas so obtained are first observed under the light microscope in order to perceive the damaged areas and possibly the growing of a crack. Cathodic metal spraying with gold facilitates further studies under the scanning electron microscope.

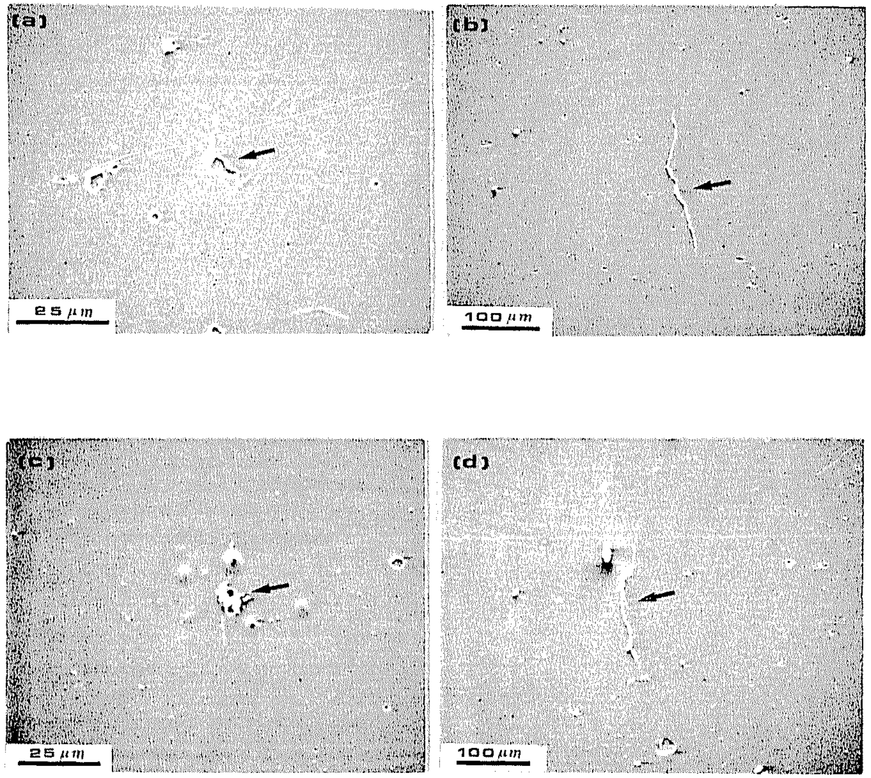

Fig 2 Three point bending results: (a) $n = 1$ type test – 25 μm long crack for 13 000 blocks; (b) $n = 1$ type test – 200 μm long crack for 39 000 blocks; (c) $n = 5$ type test – 37 μm long crack for 11 000 blocks; (d) $n = 5$ type test – 197 μm long crack for 27 000 blocks

Results and discussion

Fractographic observations

The microscopic examination of the surfaces shows that the initiation of microcracks occurs in the centre of specimen surface at Mg_2Si inclusions whose greatest dimension on the plane of observation is between 10 μm and 30 μm. Table 1 shows the results for such a crack a few microns long and gives the number of blocks required to get a semi-elliptical crack 200 μm long. This value is chosen as a criterion of initiation.

In general, the initiation crack grows out of the Mg_2Si deposits and it propagates in the matrix along a direction more or less perpendicular to the longitudinal axis of the test piece. Figures 2 and 3 illustrate the initial and final

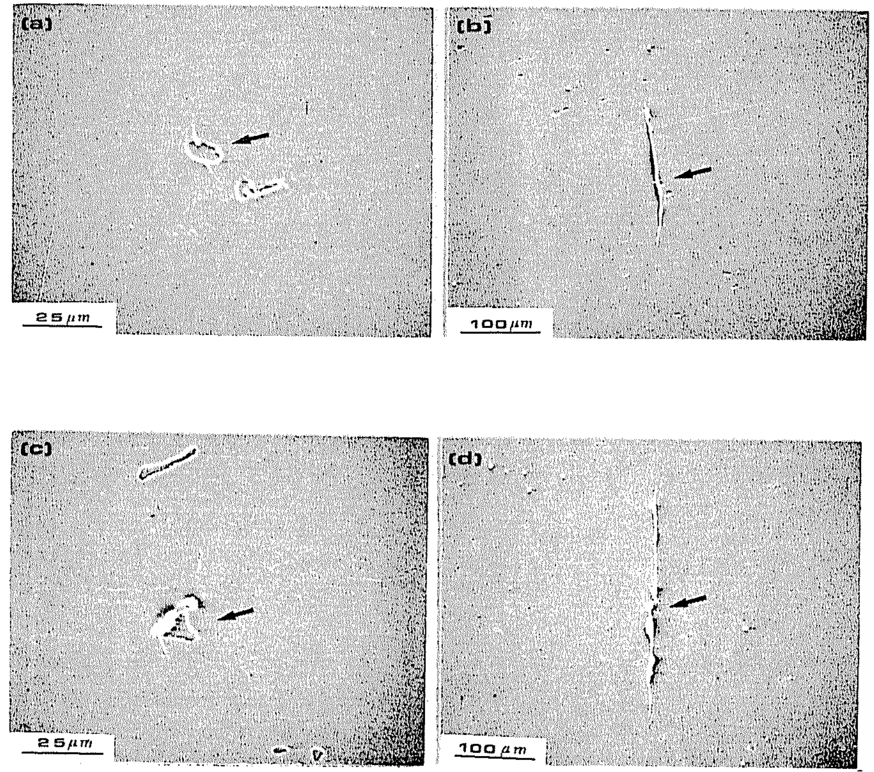

Fig 3 Three point bending results: (a) $n = 20$ type test – 10 μm long crack for 9500 blocks; (b) $n = 20$ type test – 195 μm long crack for 16 880 blocks; (c) $n = 80$ type test – 10 μm long crack for 7200 blocks; (d) $n = 80$ type test – 280 μm long crack for 10 500 blocks

stages of the propagation of a crack for the $n = 1$, $n = 5$, $n = 20$, and $n = 80$ types of tests, respectively.

The number of blocks corresponding to these various tests is given in Table 1.

Table 1 Results of the initiation tests

		Thousands of cycles for initiation	*Thousands of blocks for crack initiation*			
σ_{max} (MPa)	a (μm)	Loading with a constant amplitude $R = 0.01$	$n = 1$	$n = 5$ ($R = 0.7$)	$n = 20$	$n = 80$
365	200	10	10.5	10	9.5	7.125
		40	39	27	17	9.940

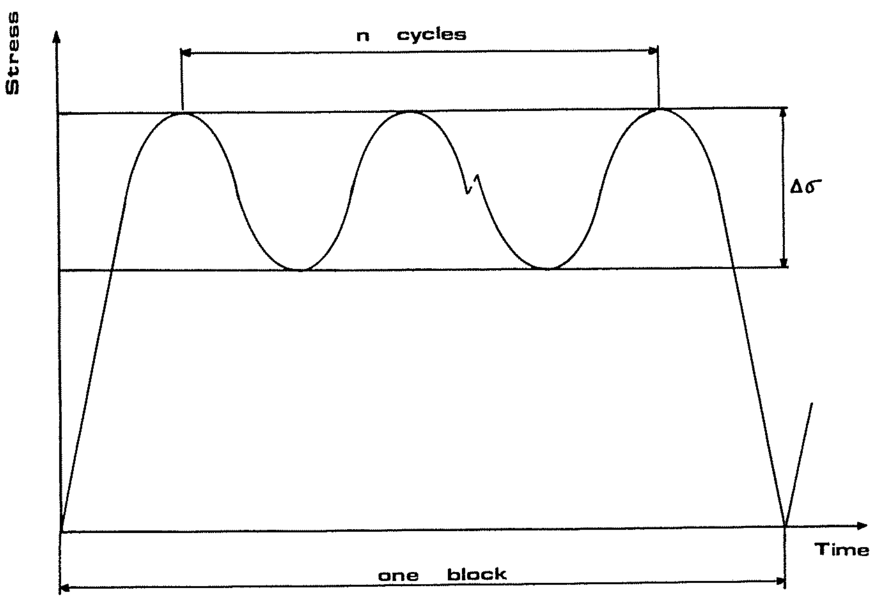

Fig 4 **Schematic: when $n = 0$, $R = 0$, and when $n = 20$ or 80, $R = 0.7$**

Figure 5 illustrates the results of the various tests in terms of n, the number of cycles for each block. One can note that the number of blocks, N, necessary to nucleate a very short crack, about 10 μm long, is almost constant whatever the number of small cycles per block may be. On the contrary, the further propagation of the short crack depends both on the main cycles and on the small cycles of the block. In the latter case, the experiment shows that there is a linear relation between the number of blocks to initiation, Na, and the number of small cycles per block, n for a given maximum stress.

The two straight lines of Fig. 5 divide the (Na, n) domain in two areas: first, an area in which only the main cycles of the block are damaging, and, secondly, an area in which the small cycles contribute to the damage as soon as a microcrack appears. It should be remembered that the small cycles of the block are not damaging when they are applied alone because their amplitude is only 110 MPa. As has been demonstrated in other works concerning initiation at a notch tip **(12)(13)**, under programmed block loading the accumulation of damage done by the small cycles and the main ones within a repeated block can be linearly expressed by equations (1), (2), and (3) below. Of course, one can write

$$\text{(Initiation)} = \text{(Nucleation)} + \text{(short crack growth)} \quad (1)$$

The equation of the first straight line giving the *nucleation* for our experimental results is

$$N = -1.7 \times 10^3 \log n + 11 \times 10^3 \quad (2)$$

Similarly, the number of blocks at the point of initiation is written

$$Na = -1.67 \times 10^3 \log n + 4 \times 10^4 \quad (3)$$

Thus we infer the equation of the propagation of the short cracks resulting from the simultaneous damage from the small cycles and the main cycles of the block

$$Np = -1.5 \times 10^4 \log n + 2.9 \times 10^4 \quad (4)$$

Crack growth rates

It is well known that the growth behaviour of a short crack is different from that of a long crack. The propagation curves that we obtained are now compared in Figs 6 and 8 for tests with a constant amplitude and with a variable amplitude of the C/n type, n being equivalent to 1, 5, 20, and 80. These results of quick propagation of short cracks below the threshold confirm the work of Pearson **(1)** and Lankford **(4)** on the aluminium alloy. In Fig. 6 the empirical curve

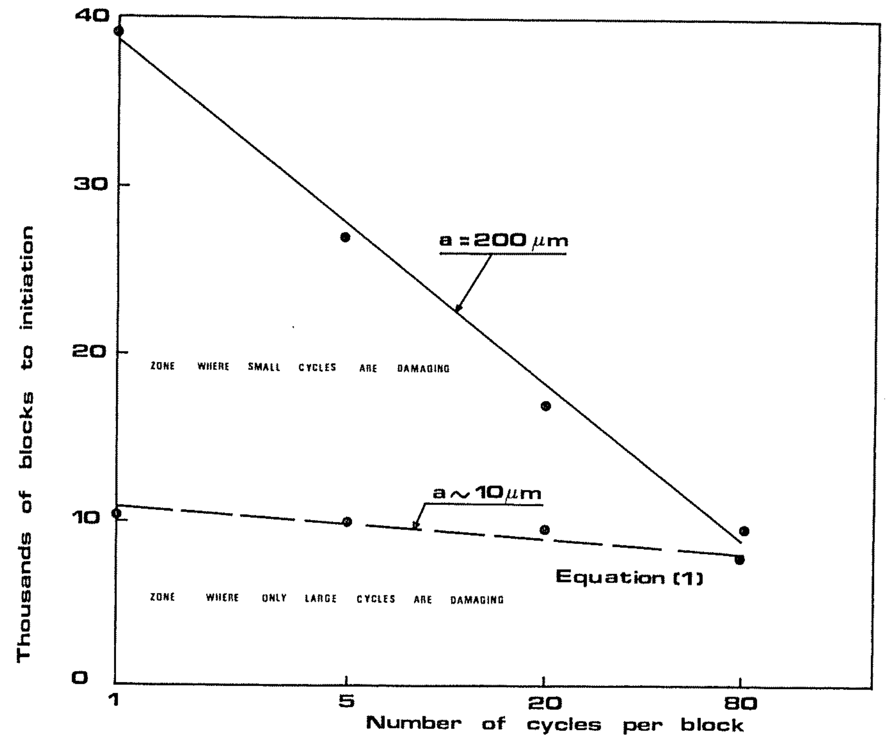

Fig 5 **Number of blocks to nucleation and initiation as a function of the number of cycles per block during three point bending tests; $\sigma_{max} = 365$ MPa**

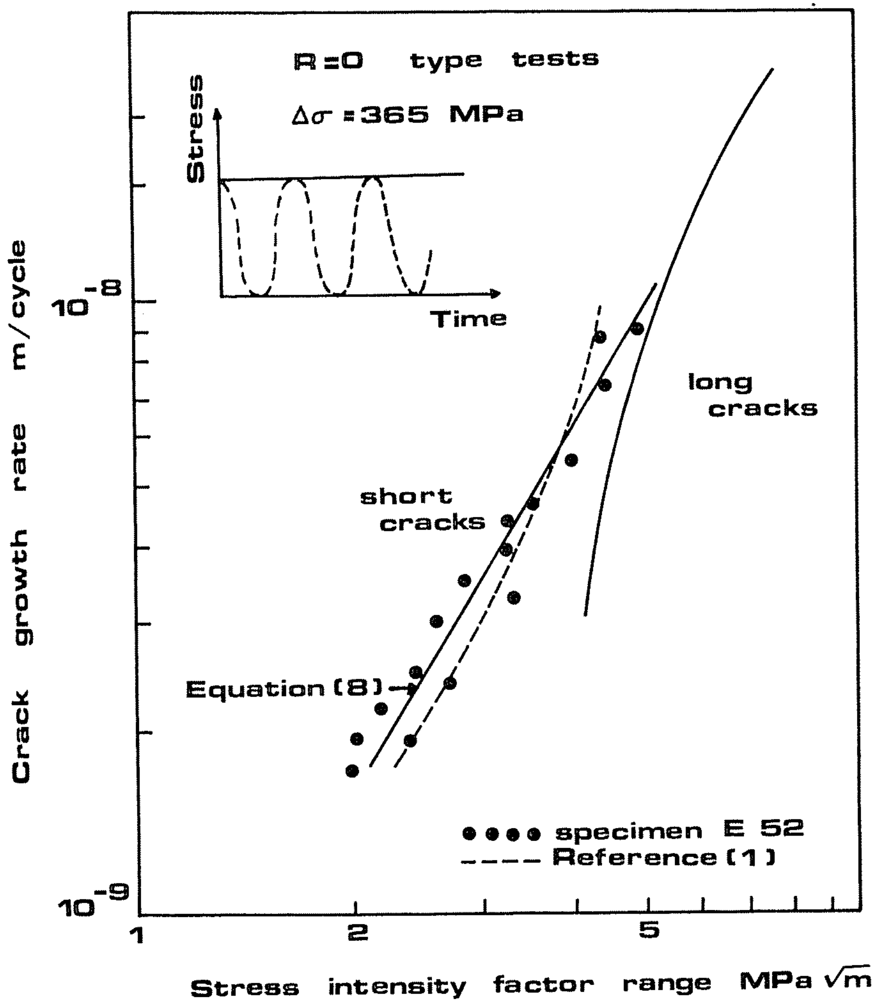

Fig 6 Three point bend test results for repeated load cycles, $R = 0$. Stress range 365 MPa

derived from Pearson's work is in good agreement with the empirical points of our tests with a $\Delta\sigma$ of 365 MPa.

The ΔK stress intensity factor in these figures was calculated with Newman's formula (**16**) for a surface elliptical crack in bending.

It may be written

$$\Delta K = HSb\sqrt{\pi \frac{a}{Q}}\, F\left(\frac{a}{t}, \frac{a}{c}, \frac{a}{b}, \theta\right) \qquad (5)$$

with the following conditions

$$0 < \frac{a}{c} \leqslant 1$$

$$0 < \frac{a}{t} \leqslant 1$$

$$c/b < 0.5$$

and

$$0 \leqslant \theta < \pi$$

Here Sb = bending stress, a = depth of the crack, c = 1/2 length of the crack on the surface and H, F, and Q = functions of a/t and a/c, t = 20 and $\theta = \pi/2$.

It must be remembered that the $2c$ length of the surface cracks is measured on replicas with a light microscope. When $2c$ is between 10 μ and 20 μ, as a first approximation the outline of the crack is considered to be semi-circular. Moreover, the crack speed during each block is determined by applying a linear accumulation between the basic cycle and the superimposed small cycles. The principle of the calculation is that two basic relationships can be written as

$$da/dN = 0.41 \times 10^{-9}(\Delta K)^{1.88} \text{ for large stress range cycles, } R = 0 \qquad (6)$$

$$da/dN = 0.41 \times 10^{-9}(\Delta K)^{2.24} \text{ for the small stress range cycles, when } n = 1 \qquad (7)$$

By superposition da/dN can be determined in terms of the above two laws of propagation for any value of n (1, 5, 20, 80, etc.), see Fig. 7. The relation for a block where n = any number becomes

$$da/dN_n = n\, da/dN_{n=1} - (n-1)da/dN_{R=0} \qquad (8)$$

The results that we obtain are added to Fig. 8 for n = 5, 20, and 80; the straight lines determined from equation (8) coincide rather well the experimental points for the various spectra.

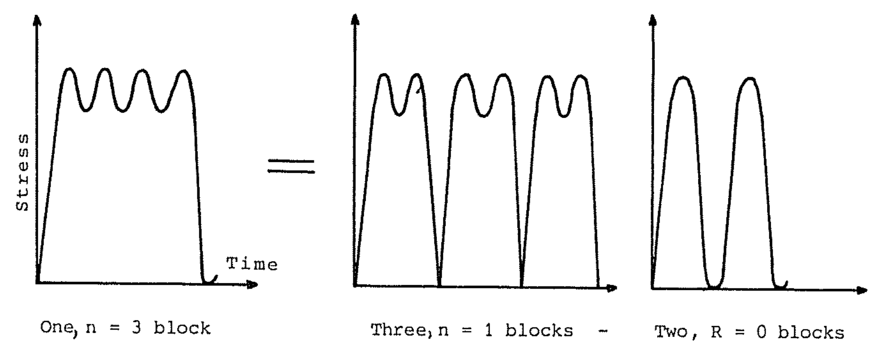

Fig 7

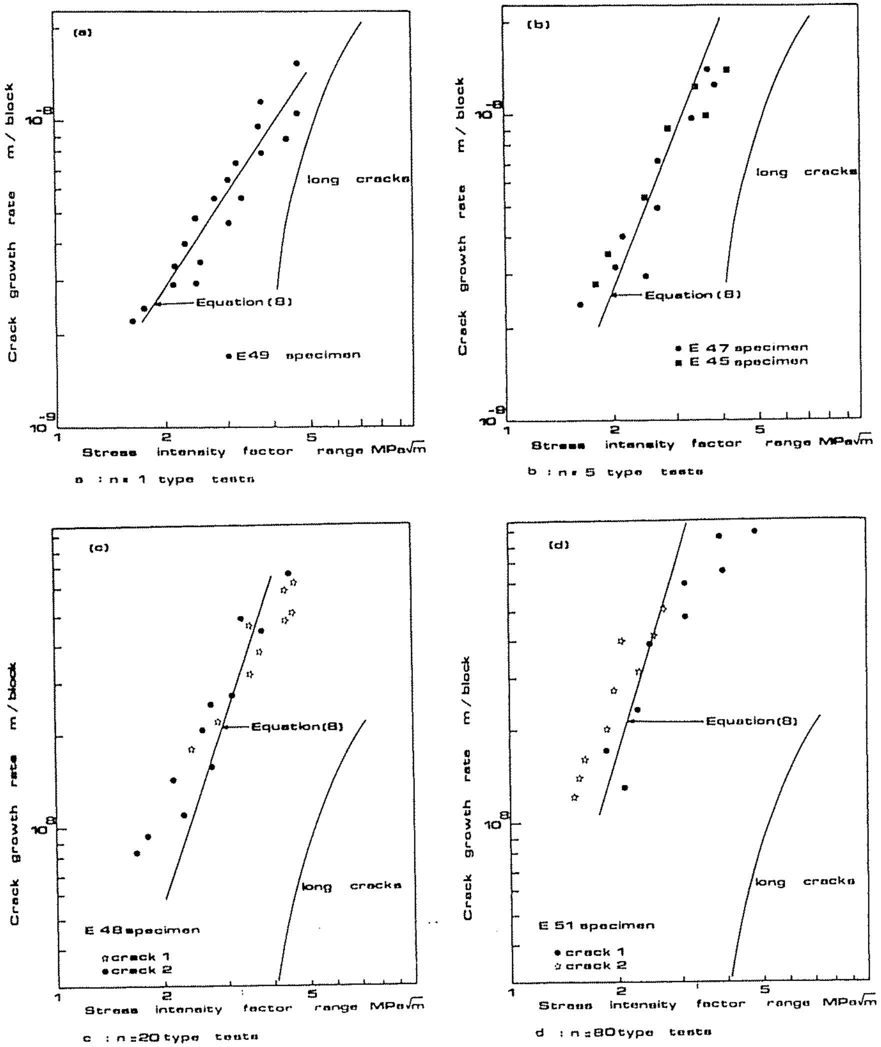

Fig 8 Three point bend test results on 7175 T 7351 alloy

It can be noticed that da/dN increases simultaneously with n for a given K and that the threshold for non-propagation is very much affected by the small n type cycles.

Mechanism of propagation for the short cracks

Observations under a light microscope on prints of the damaged area show that the microcrack grows irregularly and comes to a standstill periodically during a

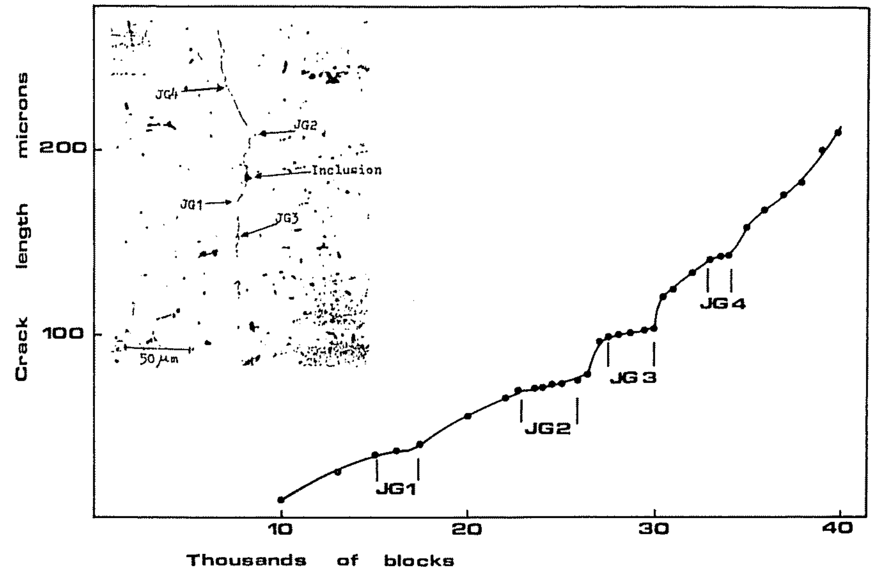

Fig 9 Fatigue crack length as a function of the number of blocks for 7175 T 7351 alloy subjected to three point bending of the $n = 1$ type

few cycles before starting its progress again. In order to explain this phenomenon we have written down the length of the crack on the surface, see Figs 9, 10, and 11, according to the number of blocks recorded for the n-type tests for n equal to 1, 20, and 80. One can note that a microcrack which initiated from an inclusion grows until it reaches the first grain boundary.

It is then slowed down by the presence of the latter; one can also note a definite time necessary for the crack to get through the grain boundary and grow into the next grain. In so far as the plastic area at the tip of the crack is limited by the nearest grain boundary, crossing the boundary implies exceeding a critical value of cumulative plastic deformation and of shearing. When the crack reaches an adequate size of between 100 μm and 130 μm it then grows continuously without being impeded by the grain boundaries through which it propagates; this aspect has also been observed by Fathualla *et al.* (**17**) on aluminium alloys.

As for the $n = 80$ test, we observed the propagation of several microcracks; two of the microcracks become predominant, while the others stopped. Figure 11 shows the nucleation of these two cracks (for a number of blocks equivalent to 7200) and their subsequent propagation. The crack that became the main one grew much more quickly and reached a length of 280 μm. The secondary crack seems to have been stopped when only 94 μm long after 10 500 blocks.

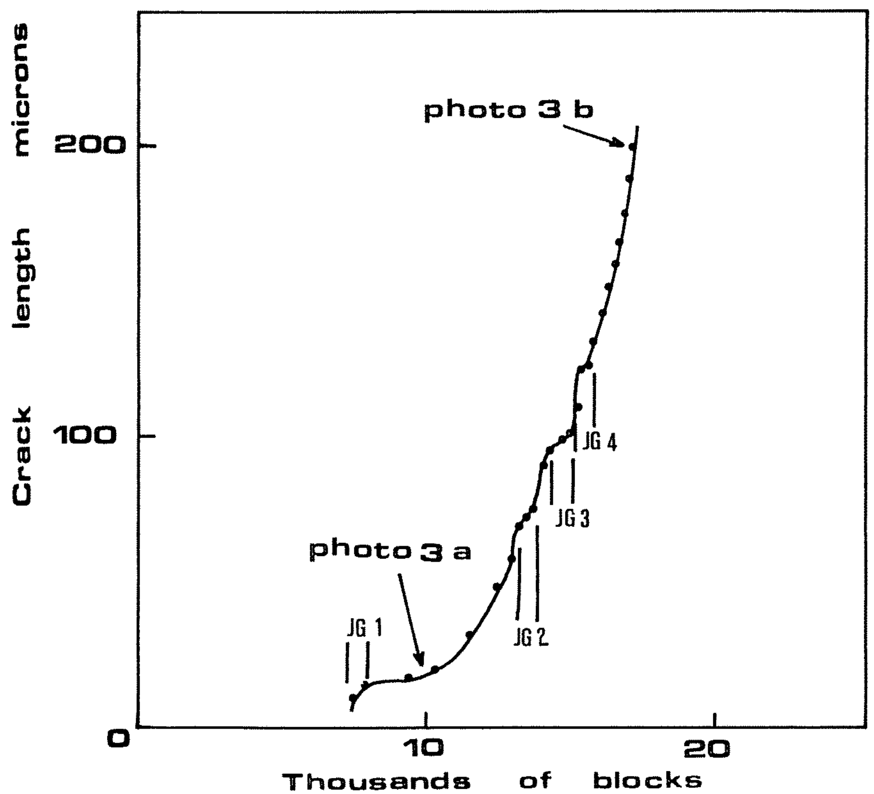

Fig 10 **Fatigue crack length as a function of the number of blocks for 7175 T 7351 alloy subjected to three point bending of the $n = 20$ type**

Conclusions

This work concerns the initiation of fatigue cracks in a 7175 T7351 aluminium alloy under complex loading.

(1) The process of initiation is one of continuous damage development whose physical nature depends on the number of cycles and the nature of the complex loading cycle.

The acoustic emission technique used in this study has made it possible to divide the initiation phase into a nucleation of a microcrack phase and a phase for the propagation of a short crack up to 200 μm in length. This criterion of initiation provides both a scientific and a technological significance.

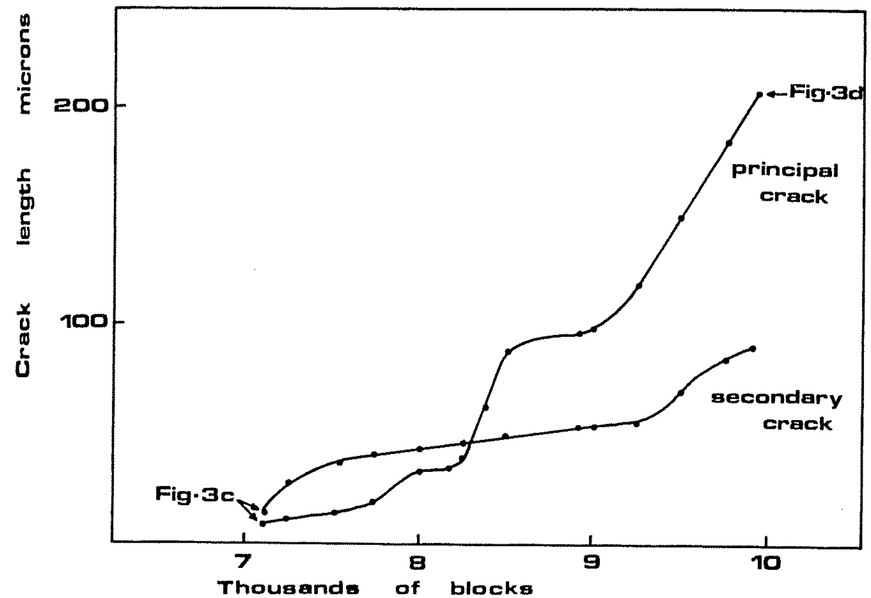

Fig 11 **Fatigue crack length as a function of the number of blocks for 7175 T 7351 alloy subjected to three point bending of the $n = 80$ type**

(2) The crack initiation phase under a ground-air-ground type of programmed loading shows that the small cycles which are limited in their damaging potential when applied alone become very damaging when they are associated with the major cycles of the block.

(3) The significance of the small cycles is related to the propagation of the short cracks on the scale of the grain size.

(4) Under programmed block loading the growth rate of short cracks, up to the point of macro-initiation, accrues in a way very different from the one anticipated by Paris's law for long cracks.

The influence of the n-type small cycles in each block is clearly revealed by a law of propagation under programmed block loading which can be described for a given loading ratio, by

$$da/dN_n = n\ da/dN_{n=1} - (n-1)\ da/dN_{R=0}$$

Knowing the growth rate of the short crack for a n-type block and the number of cycles necessary to nucleate a crack, we can calculate the number of cycles to initiation according to: number of cycles to initiation = number of cycles to nucleation + number of cycles for propagation of the short crack.

Acknowledgements

This study was financed by the Centre National de la Recherche Scientifique (CNRS), and by the Aerospace industry to whom we are most grateful.

References

(1) PEARSON, S. (1975) Initiation of fatigue cracks in commercial aluminium alloys and the subsequent propagation of very short cracks, *Engng Fracture Mech.*, **7**, 235–247.
(2) TOPPER, T. H. and EL HADDAD, M. H. (1979) Fracture mechanics analysis for short fatigue cracks, *Canad. Metall. Q.*, **18**, 207–217.
(3) KIM, Y. H., MURA, T., and FINE, M. E. (1978) Fatigue crack initiation and microcrack growth in 4140 steel, *Metall. Trans, A*, **9A**, 1679–1684.
(4) LANKFORD, J. (1982) The growth of small fatigue cracks in 7075 T 6 aluminium, *Fatigue Engng Mater. Structures*, **5**, 233–248.
(5) KUNG, C. Y. and FINE, M. E. (1979) Fatigue crack initiation and microcrack growth in 2024 T 4 and 2124 T 4 aluminium alloys, *Metall. Trans, A*, **10A**, 603–610.
(6) SHELDON, E. P., COOK, T. S., JONES, J. W., and LANKFORD, J. (1981) Some observations on small fatigue cracks in a superalloy, *Fatigue Engng Mater. Structures*, **3**, 219–228.
(7) BROWN, C. W. and HICKS, M. A. (1983) A study of short fatigue crack growth behavior in titanium alloy IMI 685, *Fatigue Engng Mater. Structures*, **6**, 67–76.
(8) DOWLING, N. E. (1982) Growth of short fatigue cracks in an alloy steel. Westinghouse R and D Center, paper 82-107–STINE–P1.
(9) GABRA, M. (1982) *Contribution à la modélisation de l'endommagement des alliages d'aluminium en fatigue par blocs programmés*, Thèse, Université de Technologie de Compiègne.
(10) GABRA, M. and BATHIAS, C. (1984) Fatigue crack initiation in aluminium alloys under programmed block loading, *Fatigue Engng Mater. Structures*, **7**, 13–27.
(11) BATHIAS, C., GABRA, M., and ALIAGA, D. (1982) Low cycle damage accumulation of aluminium alloys, *ASTM STP 770*, pp. 23–44.
(12) BOUKSIM, L. and BATHIAS, C. (1984) Etude de l'amorçage à fond d'entaille sous spectre de charge dans un alliage léger à haute résistance, *Journées Internationales de Printemps* (Société Française de Métallurgie, Paris), p. 289.
(13) BOUKSIM, L. (1985) *Amorçage des fissures de fatigue sous spectre de charge dans un alliage d'aluminium à fond d'entaille et sur des barreaux lisses.* Thèse, Université de Technologie de Compiègne.
(14) HOUSSNY EMAM, M. (1981) *Etude de l'émission acoustique associée à la déformation plastique des métaux sous sollicitation cyclique et sous l'action de l'environnement.* Thèse, Université de technologie de Compiègne.
(15) DOWLING, N. E. (1977) Cyclic stress–strain and plastic deformation aspects of fatigue crack growth, *ASTM STP 637*, p. 93.
(16) NEWMAN, J. W. Jr and RAJU, I. S. (1981) An empirical stress intensity factor equation for the surface crack, *Engng Fracture Mech.*, **15**, 185.
(17) FATHULLA, A., WEISS, B., and STICKLER, R. (1984) Initiation and propagation of short crack under cyclic loading near threshold in technical alloys, *Journées Internationales de Printemps* (Société Française de Métallurgie, Paris), p. 182.